Mass Spectrometric Identification of Aberrantly Glycosylated Human Apolipoprotein C-III Peptides in Urine from *Schistosoma mansoni*-infected Individuals*[S]

Crina I. A. Balog‡, Oleg A. Mayboroda, Manfred Wuhrer, Cornelis H. Hokke, André M. Deelder, and Paul J. Hensbergen

Schistosomiasis is a parasitic infection caused by *Schistosoma* flatworms, prime examples of multicellular parasites that live in the mammalian host for many years. Glycoconjugates derived from the parasite have been shown to play an important role in many aspects of schistosomiasis, and some of them are present in the circulation of the host. The aim of this study was to identify novel glycoconjugates related to schistosomiasis in urine of *Schistosoma mansoni*-infected individuals using a combination of glycopeptide separation techniques and in-depth mass spectrometric analysis. Surprisingly, we characterized a heterogeneous population of novel aberrantly *O*-glycosylated peptides derived from the C terminus of human apolipoprotein C-III (apoC-III) in urine of *S. mansoni*-infected individuals that were not detected in urine of non-infected controls. The glycan composition of these glycopeptides is completely different from what has been described previously for apoC-III. Most importantly, they lack sialylation and display a high degree of fucosylation. This study exemplifies the potential of mass spectrometry for the identification and characterization of *O*-glycopeptides without prior knowledge of either the glycan or the peptide sequence. Furthermore, our results indicate for the first time that as a result of *S. mansoni* infection the glycosylation of a host protein is altered. *Molecular & Cellular Proteomics 9:667–681, 2010.*

Schistosomiasis (also known as bilharzia) is one of the "neglected tropical diseases" affecting hundreds of million of people worldwide and is caused by infection with *Schistosoma* (1). Schistosomes have a complex life cycle, requiring adaptation for survival in fresh water as free-living forms and as parasites in snail intermediate hosts and vertebrate definitive hosts. Free-swimming cercariae are released from snails in water, penetrate the skin of the definitive host while shedding their tails, and transform into schistosomula. In the course of about 4–6 weeks, the schistosomula migrate via the blood circulation and become adult male or female worms. In the case of *Schistosoma mansoni*, the paired male and female worms can live in the mesenteric venules for many years. The female worms deposit hundreds of eggs each day. Many of these are transferred to the intestine and excreted with the feces to eventually continue the life cycle, but a significant fraction is trapped in the liver of the host instead. Here, they provoke eosinophilic inflammatory and granulomatous reactions, which are progressively replaced by fibrotic deposits (2, 3), damaging the overall function and integrity of the liver and thereby causing most of the morbidity associated with schistosomiasis.

During all developmental stages of the schistosome, a large variety of characteristic glycoconjugates are expressed (Ref. 4 and references cited therein), and a large number of the antibodies produced by infected subjects are directed against glycan epitopes of such schistosome glycoconjugates (5, 6). Glycoproteins produced by the eggs play an important role in the modulation of the host's immune response and in the induction of the main pathology (7–9). Some secretory glycan and glycoconjugate antigens such as the worm gut-associated circulating anodic antigen and circulating cathodic antigen (CCA)[1] are released in the circulation of the host and form the basis for diagnosis of *Schistosoma* infection using a sandwich immunoassay with anti-carbohydrate monoclonal antibodies (10, 11). Recently, the schistosome-specific multifucosylated glycan epitope recognized by a carbohydrate-specific antibody that binds to egg glycoprotein antigens has been characterized (12). Interestingly, this antibody immunocaptured free oligosaccharides containing the same multifucosylated structural elements from urine of *Schistosoma*-infected individuals (13).

From the Biomolecular Mass Spectrometry Unit, Department of Parasitology, Center of Infectious Diseases, Leiden University Medical Center, P. O. Box 9600, 2300 RC Leiden, The Netherlands

Received, November 10, 2009, and in revised form, January 5, 2010

Published, MCP Papers in Press, January 13, 2010, DOI 10.1074/mcp.M900537-MCP200

[1] The abbreviations used are: CCA, circulating cathodic antigen; apo, apolipoprotein; SCX, strong cation exchange chromatography; HILIC, hydrophilic interaction liquid chromatography; MQ, Milli-Q; RT, room temperature; Hex or H, hexose; HexNAc or N, *N*-acetylhexosamine; Fuc or F, fucose; epg, eggs/g of feces; BLAST, Basic Local Alignment Search Tool.

We hypothesized that other glycoconjugates specific for *S. mansoni* infection are present in the circulation. These might end up in the urine of infected individuals and could potentially serve as novel markers to monitor *Schistosoma* infection. To study this, we performed a comparative mass spectrometric analysis of urinary glycopeptides from *Schistosoma*-infected individuals and non-infected controls. Interestingly, we identified a set of aberrantly *O*-glycosylated, highly fucosylated peptides from human apolipoprotein C-III in urine from infected individuals but not in that from non-infected individuals.

EXPERIMENTAL PROCEDURES

Clinical Specimens, Sample Collection, and Handling—Samples were collected in areas of seasonal *S. mansoni* transmission in Africa. Consent forms were developed in the local language. Although most of the study participants could read the consent forms themselves, the purpose and contents of the study were explained in detail to the community in the local language. They were informed that the decision to participate in the survey was voluntary, and any one who wished to withdraw was free without any reprimand. Informed consent was obtained from individual adult participants, but for children, the parents or guardians consented on their behalf. Thereafter, each individual signed a consent form before commencement of any activity. All information obtained from participants was kept confidential.

Urine samples were collected in Kenya as part of the European Union Sixth Framework Program (Multi-Disciplinary Studies of Human Schistosomiasis in Uganda, Kenya and Mali: New Perspectives on Morbidity, Immunity, Treatment and Control (MUSTSchistUKEMA)). Ethical clearance was obtained from the Kenya National ethics committee, and the study was presented to the Danish National Committee on Biomedical Research Ethics in Denmark. The urine samples were collected in 50-ml Falcon tubes (BD Biosciences) randomly at different time points of the day, kept on ice immediately after collection, and stored at −20 °C when the day's field activities were over. The samples were transported on dry ice to The Netherlands, aliquoted in 2.2-ml storage plates (Westburg, Leusden, The Netherlands), and stored at −20 °C until use. Urine samples were analyzed from six infected and four non-infected individuals. All analyzed urine samples were given a MS analysis number (non-infected: 10966, female, 34 years; 10967, male, 33 years; 10968, male, 43 years; and 10410, male, 70 years; infected: 10411, male, 68 years; 10412, female, 7 years; 10413, male, 43 years; 22824, female, 19 years; 22828, male, 10 years; and 22830, male, 14 years). Urine samples were analyzed using CCA strips as described previously (14). Infection was recorded as eggs/g of feces (epg) using two Kato-Katz thick smears per stool sample (15). The determined egg count and measured CCA values were as follows: 10411, 10 epg and CCA of 1; 10412, 900 epg and CCA of 3; 10413, 160 epg and CCA of 3; 22824, 205 epg and CCA of 3; 22828, 4565 epg and CCA of 3; and 22830, 830 epg and CCA of 3. Samples 10966, 10967, 10968, and 10410 were egg-negative and CCA-negative.

The serum samples were provided from a study that was carried out in the village of Ndombo, Senegal (population ~4,000) situated near Richard Toll. The study design, epidemiology, and sample collection have been described in detail elsewhere (16, 17). Shortly, venous (adults) or capillary (children less than 5 years of age) blood samples were collected, allowed to stand at room temperature for 1 h, and centrifuged at 1500 rpm. The serum was carefully removed and stored frozen at −15 °C. The serum samples were transported on dry ice to The Netherlands, aliquoted in 1.5-ml tubes (Eppendorf, Hamburg, Germany), and stored at −80 °C until use. In total, six serum samples were analyzed (three infected and three non-infected). All serum samples were given a MS analysis number (non-infected: 11254, female, 33 years; 11255, male, 30 years; and 11251, male, 37 years; infected: 11250, female, 13 years, egg count of 8147 epg; 11249, female, 50 years, egg count of 287 epg; and 11252, male 11 years, egg count of 6080 epg).

Isolation of Urinary Peptides—Urines were centrifuged at 1500 × *g* for 10 min at room temperature (RT), and the pellet was discarded. Three volumes of cold ethanol were then added to 1 volume of urine followed by gentle mixing, and urinary proteins were precipitated overnight at −20 °C. The samples were subsequently spun for 45 min at 10,000 rpm, and the precipitated proteins were removed. The samples were then completely dried and stored at −20 °C.

Strong Cation Exchange Chromatography (SCX)—Samples were resuspended in 500 μl of Solvent A (10 mM KH_2PO_4 (pH 2.9), 20% ACN). 100 μl of each sample was injected on a PolySULFOETHYL A column (100 × 2.1 mm, 3 μm, 300 Å; PolyLC, Columbia, MD) at a flow rate of 0.2 ml/min using an ÄKTA™Purifier (GE Healthcare) controlled by UNICORN software. After washing for 3.5 min with 100% Solvent A, peptides were eluted using a linear gradient from 30% Solvent B (500 mM KCl, 10 mM KH_2PO_4 (pH 2.9), 20% ACN) to 100% Solvent B in 45 min. A total number of 16 fractions with a volume of 0.5 ml (2.5 min/fraction) were collected.

Hydrophilic Interaction Liquid Chromatography (HILIC)—Fractions 5 and 6 from five consecutive SCX fractionations from the same urine sample were pooled, lyophilized, and resuspended in 1 ml of Solvent C (50 mM ammonium formate (pH 4.4) containing 70% ACN). The sample was then loaded on a TSK-gel Amide-80 column (4.6-mm inner diameter × 25 cm long; particle size, 5 μm; Tosoh Bioscience, Stuttgart, Germany) at a flow rate of 0.4 ml/min using an ÄKTAPurifier controlled by UNICORN software. Peptides were eluted using a linear gradient of 12.5–50% Solvent D (50 mM ammonium formate) in 60 min. UV absorbance was measured at 215 nm. A total of 33 fractions with a volume of 1 ml (2.5 min/fraction) were collected, freeze-dried, and resuspended in 40 μl of 0.1% TFA.

MALDI-TOF Mass Spectrometry—Dried and reconstituted samples were desalted using a C_{18} ZipTip™ (Millipore, Billerica, MA) following the manufacturer's instructions. Peptides were eluted with 1.5 μl of 5 mg/ml 2,5-dihydroxybenzoic acid (dissolved in 50:50 ACN:MQ water containing 0.1% TFA) directly onto a stainless steel MALDI target plate (Bruker Daltonics, Bremen, Germany) and allowed to dry.

MALDI-TOF mass analyses were performed on an Ultraflex II time-of-flight mass spectrometer controlled by the FlexControl 3.0 software package (Bruker Daltonics). The MS acquisitions were performed in positive ion reflectron mode at a laser frequency of 50 Hz. The scanner *m/z* range was up to 5000, and the matrix suppression (deflection) mode was up to *m/z* 400. For the MS/MS analysis, precursors were accelerated and selected in a time ion gate after which fragments arising from metastable decay were further accelerated in the LIFT cell, and their *m/z* values were analyzed after passing the ion reflector.

Nano-LC ESI MS/MS—Nanoflow LC was performed on an Ultimate LC system (Dionex, Sunnyvale, CA). A volume of 10 μl of sample was injected onto a C_{18} PepMap™ 0.3 × 5-mm trapping column (Dionex) and washed with 100% A (2% ACN in 0.1% formic acid in MQ water, v/v) at 20 μl/min for 40 min. Following valve switching, peptides were separated on a C_{18} PepMap 75-μm × 150-mm column (Dionex) at a constant flow of 200 nl/min. The peptide elution gradient was from 10 to 60% B (95% ACN in 0.1% formic acid in MQ water, v/v) over 50 min. The nanoflow LC system was coupled to an HCTultra IonTrap (Bruker Daltonics) using a nanoelectrospray ionization source. The spray voltage was set at 1.2 kV, and the temperature of the heated capillary was set to 165 °C. Eluting peptides were analyzed using the data-dependent MS/MS mode over a 300–1500 *m/z* range. The five most abundant ions in an MS spectrum were selected for MS/MS

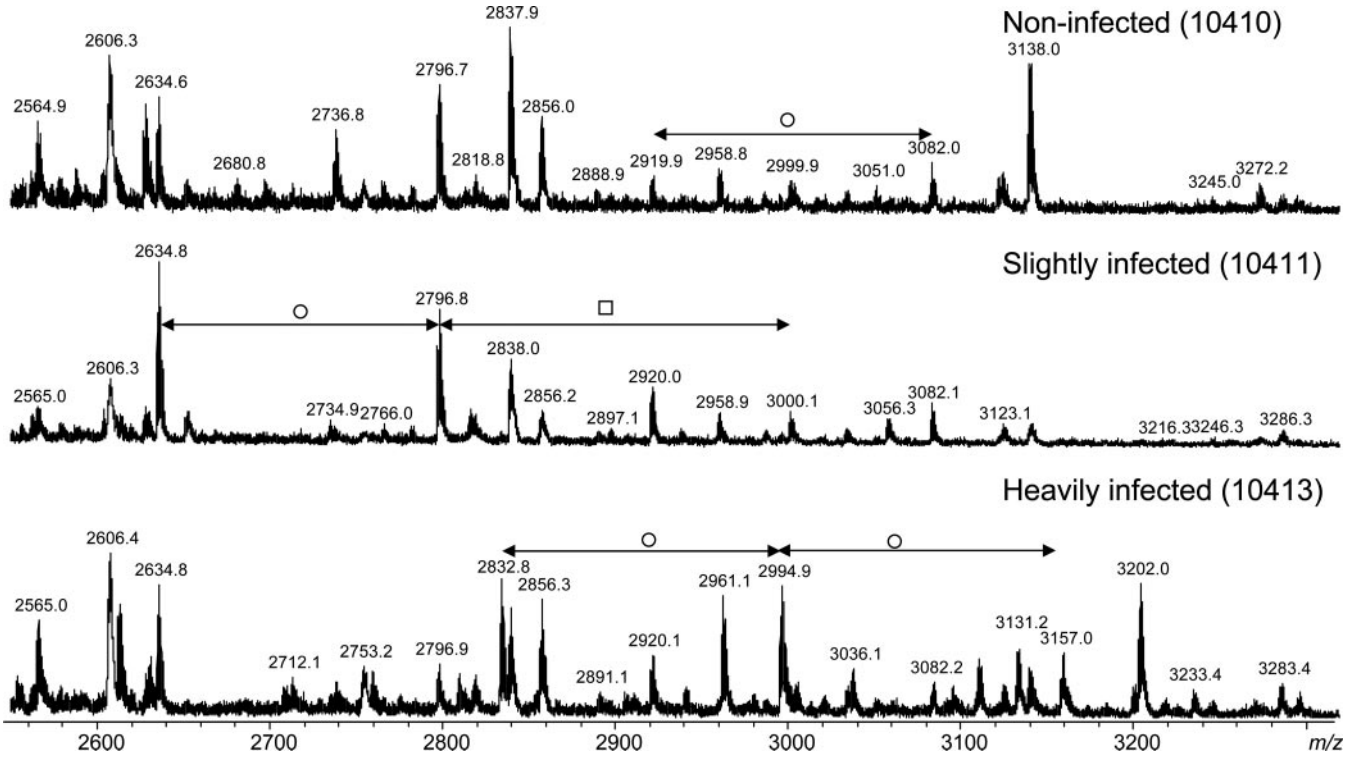

FIG. 1. **MALDI-TOF MS analysis of urinary (glyco)peptides from control and *S. mansoni*-infected individuals.** Urinary peptides were separated using strong cation exchange chromatography, and collected fractions were analyzed using MALDI-TOF MS. *Numbers* refer to MS numbers given to the samples. *Open square*, *N*-acetylhexosamine; *open circle*, hexose.

analysis by collision-induced dissociation using helium as the collision gas. Additionally, for MS^3 experiments, fragments of interest observed in an MS/MS spectrum were manually isolated and fragmented.

MALDI-TOF MS of Full-length Apolipoprotein C-III from Serum—Apolipoprotein C-III isoforms in serum were measured by MALDI-TOF MS according to Nelsestuen *et al.* (18). Briefly, serum (0.8 μl) was diluted with MQ water:ACN:TFA (20 μl, 95:5:0.1) and allowed to stand for 1 h at RT. The hydrophobic compounds were then extracted with a reverse phase C_{18} ZipTip (Millipore) following the manufacturer's instructions. Following standard procedures, 1 μl of the eluted sample in MQ water:ACN:TFA (25:75:0.1) was applied to the MALDI target along with sinapinic acid (1 μl of saturated solution in MQ water:ACN:TFA, 50:50:0.1). Uniform crystallization was achieved by manual mixing of the sample with the pipette tip. The sample was dried and analyzed on an Ultraflex II MALDI-TOF mass spectrometer (Bruker Daltonics) operating in the linear positive ion mode. Two thousand laser shots were collected for each sample.

Trypsin Digestion—Five microliters of a 10% buffered aqueous solution of human apolipoprotein C-III (Sigma-Aldrich) was diluted with 10 μl of 50 mM ammonium bicarbonate. Then, 0.5 μl of 100 mM dithiothreitol was added, and samples were incubated for 30 min at 56 °C. Subsequently, 5 μl of 55 mM iodoacetamide was added, and samples were kept at RT for 20 min. Tryptic digestion was then performed by adding 5 μg of trypsin (sequencing grade modified trypsin, Promega, Madison, WI) and incubating overnight at 37 °C.

RESULTS

Analysis of Glycopeptides in Urine from S. mansoni*-infected Individuals and Non-infected Controls*—Urine samples collected from *S. mansoni*-infected individuals and non-infected controls were subjected to organic precipitation to deplete large proteins. Subsequently, samples were desalted on a reverse phase cartridge and fractionated by strong cation exchange chromatography. Following desalting, every fraction was analyzed using MALDI-TOF MS. Because we were specifically interested in the analysis of schistosomiasis-related glycopeptides, we primarily focused on the higher *m/z* ranges. A representative MALDI-TOF mass spectrum from one SCX fraction from both non-infected and infected individuals is seen in Fig. 1. In the *S. mansoni*-infected individuals, we observed several signals between *m/z* 2500 and *m/z* 3500 that were not detected in the non-infected individuals. Furthermore, between several of the masses present in the individual spectra, mass differences corresponding to monosaccharides were evident, indicating the presence of a series of glycopeptides in these fractions. The fraction from the heavily infected individual was further analyzed with nano-LC-ion trap MS. The five most abundant ions in every MS spectrum were automatically selected for MS/MS, and spectra were searched for the presence of glycan-specific oxonium ions (*m/z* 366 ($[Hex_1\text{-}HexNAc_1 + H]^+$) and 512 ($[Fuc_1\text{-}Hex_1\text{-}HexNAc_1 + H]^+$). An MS/MS spectrum of one of the glycoconjugates observed at *m/z* 1068.2 $[M + 3H]^{3+}$ is given in Fig. 2. This peptide was observed at *m/z* 3202.0 in the MALDI-TOF mass spectrum from the SCX fraction from the heavily infected individual but not in the slightly and non-infected samples (Fig. 1). The MS/MS frag-

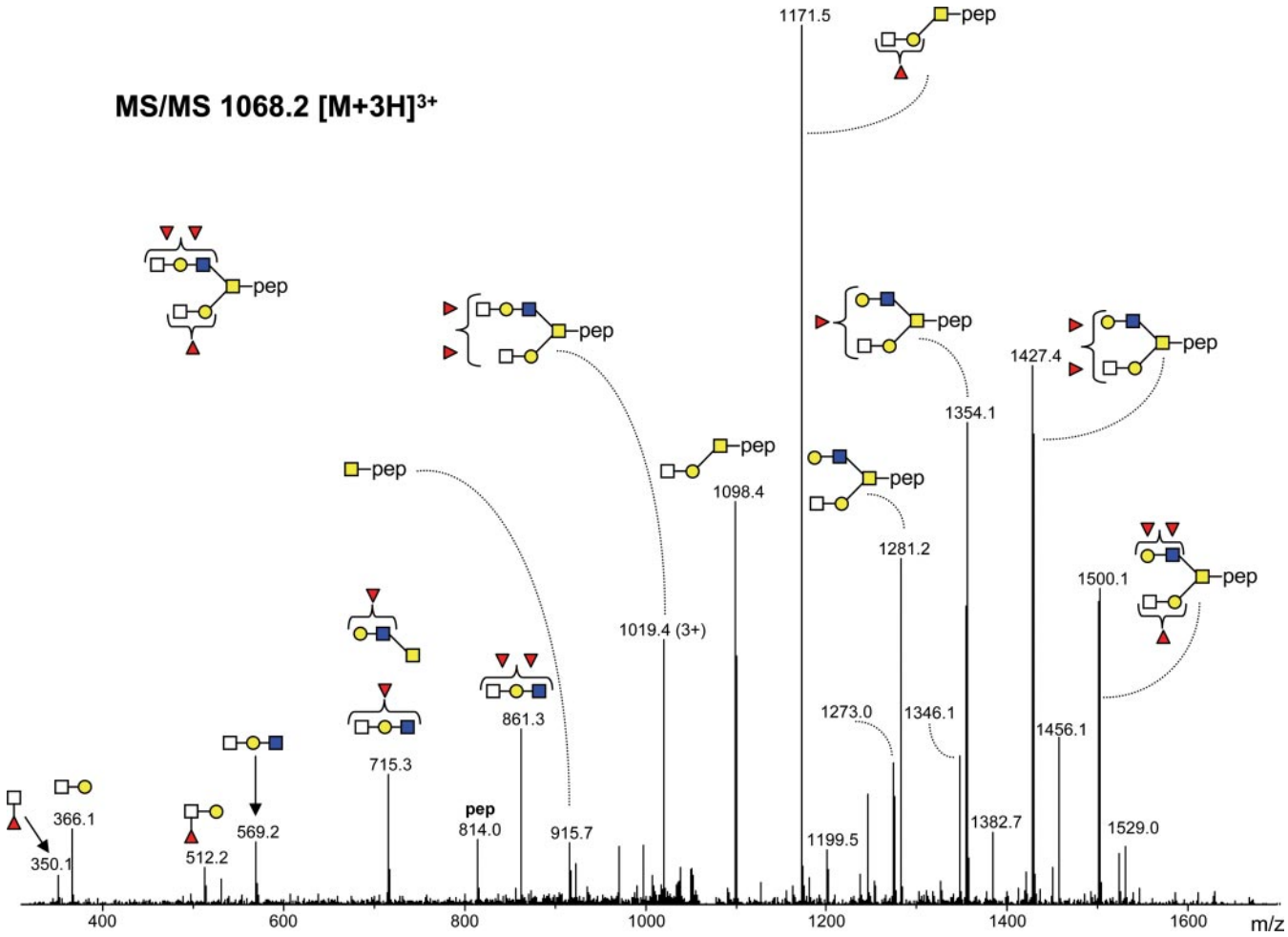

FIG. 2. **MS/MS fragmentation of a glycopeptide present in urine from a *S. mansoni*-infected individual.** Urinary peptides from an *S. mansoni*-infected individual were separated using strong cation exchange chromatography. Fractions containing glycopeptides were analyzed using LC-ion trap MS, and glycopeptides were fragmented using collisional-induced dissociation. Shown is the MS/MS spectrum from a glycopeptide *m/z* 1068.2 $[M + 3H]^{3+}$ present only in the infected individual with a glycan moiety composed of $H_2N_4F_3$. If not indicated differently, all ions containing the peptide moiety (*pep*) are doubly charged, and those lacking the peptide moiety are singly charged. No monosaccharide linkage information is obtained. *Red triangle*, fucose; *yellow circle*, galactose; *blue square*, *N*-acetylglucosamine; *yellow square*, *N*-acetylgalactosamine; *open square*, *N*-acetylhexosamine.

mentation in Fig. 2 demonstrated a clear glycopeptide fragmentation pattern as shown by the characteristic presence of highly abundant singly charged glycan-specific oxonium ions at *m/z* 350.1 ($[Fuc_1\text{-}HexNAc_1 + H]^+$), 366.1 ($[Hex_1\text{-}HexNAc_1 + H]^+$), 512.2 ($[Fuc_1\text{-}Hex_1\text{-}HexNAc_1 + H]^+$), 569.2 ($[Hex_1\text{-}HexNAc_2 + H]^+$), 715.3 ($[Fuc_1\text{-}Hex_1\text{-}HexNAc_2 + H]^+$), and 861.3 ($[Fuc_2\text{-}Hex_1\text{-}HexNAc_2 + H]^+$).

In addition, sequential losses of glycosyl residues from the parent ion were observed. The strong signal at *m/z* 1500.1 $[M + 2H]^{2+}$ indicates the initial loss of a HexNAc residue, suggesting the presence of a terminal HexNAc residue. Subsequently, consecutive losses of three fucose residues were observed (*m/z* 1427.4 $[M + 2H]^{2+}$, *m/z* 1354.1 $[M + 2H]^{2+}$, and *m/z* 1281.2 $[M + 2H]^{2+}$). Similarly, the losses of up to three fucoses from the parent ion were observed (*m/z* 1529.0 $[M + 2H]^{2+}$, *m/z* 1456.1 $[M + 2H]^{2+}$, and *m/z* 1382.7 $[M + 2H]^{2+}$). No initial loss of a Hex was observed, suggesting that only HexNAc and Fuc residues occupy terminal positions. However, after the loss of a HexNAc and a Fuc residue, we also observed the loss of Hex residues as exemplified by ions at *m/z* 1273.0 and *m/z* 1346.1 (Table I). After the initial cascade of one HexNAc and three Fuc losses, we observed subsequent losses of a Hex at *m/z* 1199.5 $[M + 2H]^{2+}$, a HexNAc at *m/z* 1098.4 $[M + 2H]^{2+}$, a $Hex_1\text{-}HexNAc_1$ at *m/z* 915.7 $[M + 2H]^{2+}$, and a HexNAc at *m/z* 814.0 $[M + 2H]^{2+}$.

The absence of large oxonium ions containing more than two HexNAc residues or more than one Hex element indicates a branched glycan structure. The $HexNAc_1\text{-}Hex_1\text{-}HexNAc_1$ (H_1N_2) element is observed as a fragment at *m/z* 569.2 $[M + H]^+$ and as $(HexNAc_1\text{-}Hex_1\text{-}HexNAc_1)\text{-}Fuc_2$ ($H_1N_2F_2$) at *m/z* 861.3 $[M + H]^+$, indicating that one arm of the glycan is $H_1N_2F_2$. Similarly, the signal at *m/z* 512.2 $[M + H]^+$ is indic-

TABLE I

Overview of aberrantly glycosylated human apolipoprotein C-III peptides identified in this study

Urinary peptides from *S. mansoni*-infected and non-infected individuals were separated using strong cation exchange chromatography. Fractions from urine of the infected individuals containing aberrantly glycosylated peptides from apoC-III were analyzed using LC-ion trap MS/MS, and the glycan composition and peptide backbone were assigned based on the fragment ions. Corresponding fractions from non-infected individuals were analyzed similarly. Sample numbers correspond to MS numbers assigned at the beginning of the study. The previously described glycan composition of the three human apoC-III glycoforms is also shown. y_8^* refers to the peptide fragment PEVRPTSA. Double charged ions are indicated as [M+2H]. n.a., not applicable; pep, peptide moiety.

Samples	*m/z* of aberrant apoC-III glycopeptides	Fragment ions	Peptide sequence	Glycan composition
Human apoC-III				
ApoC-III$_0$	n.a.			H_1N_1[a]
ApoC-III$_1$	n.a.			$H_1N_1S_1$[a]
ApoC-III$_2$	n.a.			$H_1N_1S_2$[a]
Non-infected urines				
10966	Not detected			
10967	Not detected			
10968	Not detected			
10410	Not detected			
Infected urines				
10411	939.3 $[M + 3H]^{3+}$	350.1 (N_1F_1); 366.1 (H_1N_1); 512.2 ($H_1N_1F_1$); 569.2 (H_1N_2); 715.4 ($H_1N_2F_1$); 693.7 (pep; [M + 2H]); 795.2 (pep-N_1; [M + 2H]); 977.5 (pep-H_1N_2; [M + 2H]); 1079.0 (pep-H_1N_3; [M + 2H]); 1160.0 (pep-H_2N_3; [M + 2H]); 1233.0 (pep-$H_2N_3F_1$; [M + 2H]); 1261.6 (pep-H_2N_4; [M + 2H]); 1306.1 (pep-$H_2N_3F_2$; [M + 2H]); 1334.0 (pep-H_2N_4F; [M + 2H])	WDLDPEVRPTSA	$H_2N_4F_2$
	995.8 $[M + 3H]^{3+}$	350.1 (N_1F_1); 366.1 (H_1N_1); 512.2 ($H_1N_1F_1$); 715.4 ($H_1N_2F_1$); 778.2 (pep; [M + 2H]); 879.8 (pep-N_1; [M + 2H]); 1062.5 (pep-H_1N_2; [M + 2H]); 1135.4 (pep-$H_1N_2F_1$; [M + 2H]);1163.8 (pep-H_1N_3; [M + 2H]); 1237.0 (pep-$H_1N_3F_1$; [M + 2H]); 1245.0 (pep-H_2N_3; [M + 2H]); 1318.0 (pep-$H_2N_3F_1$; [M + 2H]); 1347.0 (pep-H_2N_4; [M + 2H]); 1391.0 (pep-$H_2N_3F_2$; [M + 2H]); 1420.5 (pep-$H_2N_4F_1$; [M + 2H])	WDLDPEVRPTSAVA	$H_2N_4F_2$
	1019.7 $[M + 3H]^{3+}$	350.1 (N_1F_1); 366.1 (H_1N_1); 512.1 ($H_1N_1F_1$); 569.2 (H_1N_2); 715.4 ($H_1N_2F_1$); 814.1 (pep; [M + 2H]); 915.7 (pep-N_1; [M + 2H]); 1098.5 (pep-H_1N_2; [M + 2H]); 1171.5 (pep-$H_1N_2F_1$; [M + 2H]); 1200.0 (pep-H_1N_3; [M + 2H]); 1273.0 (pep-$H_1N_3F_1$; [M + 2H]); 1281.1 (pep-H_2N_3; [M + 2H]); 1354.1 (pep-$H_2N_3F_1$; [M + 2H]); 1427.2 (pep-$H_2N_3F_2$; [M + 2H]); 1626.8 (pep); 1830.7 (pep-N); 1992.8 (pep-H_1N_1); 2138.8 (pep-$H_1N_1F_1$); 2342.8 (pep-$H_1N_2F_2$)	WDLDPEVRPTSAVAA	$H_3N_3F_2$
10412	1044.9 $[M + 3H]^{3+}$	350.1 (N_1F_1); 366.1 (H_1N_1); 512.2 ($H_1N_1F_1$); 715.4 ($H_1N_2F_1$); 861.3 ($H_1N_2F_2$); 778.2 (pep; [M + 2H]); 879.8 (pep-N_1; [M + 2H]); 1062.9 (pep-H_1N_2; [M + 2H]); 1136.0 (pep-$H_1N_2F_1$; [M + 2H]); 1209.0 (pep-$H_1N_2F_2$; [M + 2H]); 1217.0 (pep-$H_2N_2F_1$; [M + 2H]); 1237.0 (pep-$H_1N_3F_1$; [M + 2H]); 1245.0 (pep-H_2N_3; [M + 2H]); 1310.6 (pep-$H_1N_3F_2$; [M + 2H]); 1318.0 (pep-$H_2N_3F_1$; [M + 2H]); 1391.0 (pep-$H_2N_3F_2$; [M + 2H]); 1464.7 (pep-$H_2N_3F_3$; [M + 2H])	WDLDPEVRPTSAVA	$H_2N_4F_3$
	995.8 $[M + 3H]^{3+}$	350.1 (N_1F_1); 366.1 (H_1N_1); 512.2 ($H_1N_1F_1$); 715.4 ($H_1N_2F_1$)	WDLDPEVRPTSAVA	$H_2N_4F_2$
10413	871.5 $[M + 3H]^{3+}$	350.1 (N_1F_1); 366.1 (H_1N_1); 512.2 ($H_1N_1F_1$); 977.5 (pep-H_1N_2; [M + 2H]); 1050.5 (pep-$H_1N_2F_1$; [M + 2H]); 1124.0 (pep-$H_1N_2F_2$; [M + 2H]); 1131.9 (pep-$H_2N_2F_1$; [M + 2H]); 1159.5 (pep-H_2N_3; [M + 2H]); 1205.5 (pep-$H_2N_2F_2$; [M + 2H]); 1233.0 (pep-$H_2N_3F_1$; [M + 2H])	WDLDPEVRPTSA	$H_2N_4F_3$
	987.8 $[M + 3H]^{3+}$	350.1 (N_1F_1); 366.1 (H_1N_1); 512.2 ($H_1N_1F_1$); 715.4 ($H_1N_2F_1$); 693.7 (pep; [M + 2H]); 795.2 (pep-N_1; [M + 2H]); 977.5 (pep-H_1N_2; [M + 2H]); 1050.0 (pep-$H_1N_2F_1$; [M + 2H]); 1124.1(pep-$H_1N_2F_2$; [M + 2H]); 1160.0 (pep-H_2N_3; [M + 2H]); 1233.0 (pep-$H_2N_3F_1$; [M + 2H]); 1261.5 (pep-H_2N_4; [M + 2H]); 1306.1 (pep-$H_2N_3F_2$; [M + 2H]); 1335.6 (pep-$H_2N_4F_1$; [M + 2H]); 1379.6 (pep-$H_2N_3F_3$; [M + 2H]); 1408.1 (pep-$H_2N_4F_2$; [M + 2H])	WDLDPEVRPTSA	$H_2N_4F_3$
10413	1068.2 $[M + 3H]^{3+}$	350.1 (N_1F_1); 366.1 (H_1N_1); 512.2 ($H_1N_1F_1$); 569.2 (H_1N_2); 658.2 ($H_1N_1F_2$); 715.3 ($H_1N_2F_1$); 861.3 ($H_1N_2F_2$); 814.0 (pep; [M + 2H]); 915.7 (pep-N_1; [M + 2H]); 1098.4 (pep-H_1N_2; [M + 2H]); 1171.5 (pep-$H_1N_2F_1$; [M + 2H]); 1244.6 (pep-$H_1N_2F_2$; [M + 2H]); 1273.0 (pep-$H_1N_3F_1$; [M + 2H]); 1281.2 (pep-H_2N_3; [M + 2H]); 1346.1 (pep-$H_1N_3F_2$; [M + 2H]); 1354.1 (pep-$H_2N_3F_1$; [M + 2H]); 1418.7 (pep-$H_1N_3F_3$; [M + 2H]); 1427.4 (pep-$H_2N_3F_2$; [M + 2H]); 1456.1 (pep-$H_2N_4F_1$; [M + 2H]); 1500.1 (pep-$H_2N_3F_3$; [M + 2H]); 1529.0 (pep-$H_2N_4F_2$; [M + 2H])	WDLDPEVRPTSAVAA	$H_2N_4F_3$

TABLE I—*continued*

Samples	*m/z* of aberrant apoC-III glycopeptides	Fragment ions	Peptide sequence	Glycan composition
	1214.8 $[M + 3H]^{3+}$	350.1 (N_1F_1); 366.1 (H_1N_1); 512.2 ($H_1N_1F_1$); 658 ($H_1N_1F_2$); 715.4 ($H_1N_2F_1$); 861.3 ($H_1N_2F_2$); 1062.9 (pep-H_1N_2; $[M + 2H]$); 1136.0 (pep-$H_1N_2F_1$; $[M + 2H]$); 1165.0 (pep-H_1N_3; $[M + 2H]$); 1245.0 (pep-H_2N_3; $[M + 2H]$); 1318.0 (pep-$H_2N_3F_1$; $[M + 2H]$); 1391.0 (pep-$H_2N_3F_2$; $[M + 2H]$); 1419.7 (pep-$H_2N_4F_1$; $[M + 2H]$); 1493.7 (pep-$H_2N_4F_2$; $[M + 2H]$); 1567.2 (pep-$H_2N_4F_3$; $[M + 2H]$); 1574.5 (pep-$H_3N_4F_2$; $[M + 2H]$); 1647.6 (pep-$H_3N_4F_3$; $[M + 2H]$); 1721.1 (pep-$H_3N_4F_4$; $[M + 2H]$)	WDLDPEVRPTSAVA	H_3N5F_4
22824	802.8 $[M + 3H]^{3+}$	350.1 (N_1F_1); 366.0 (H_1N1); 512.0 ($H_1N_1F_1$); 876.2 (pep-H_1N_1; $[M + 2H]$); 948.7 (pep-$H_1N_1F_1$; $[M + 2H]$); 1021.7 (pep-$H_1N_1F_2$; $[M + 2H]$);1058.7 (pep-H_2N_2; $[M + 2H]$); 1131.7 (pep-$H_2N_2F_1$; $[M + 2H]$)	WDLDPEVRPTSA	$H_2N_2F_2$
	1204.2 $[M + 2H]^{2+}$	350.1 (N_1F_1); 366.0 (H_1N_1); 512.0 ($H_1N_1F_1$); 875.7 (pep-H_1N_1; $[M + 2H]$); 948.8 (pep-$H_1N_1F_1$; $[M + 2H]$); 1022.2 (pep-$H_1N_1F_2$; $[M + 2H]$);1058.7 (pep-H_2N_2; $[M + 2H]$); 1131.5 (pep-$H_2N_2F_1$; $[M + 2H]$); 1385.5 (pep); 1588.6 (pep-N); 1750.7 (pep-H_1N_1); 1896.7 (pep-$H_1N_1F_1$); 2042.7 (pep-$H_1N_1F_2$)	WDLDPEVRPTSA	$H_2N_2F_2$
	851.5 $[M + 3H]^{3+}$	350.1 (N_1F_1); 366.0 (H_1N_1); 512.0 ($H_1N_1F_1$); 658.1 ($H_1N_1F_2$); 875.7 (pep-H_1N_1; $[M + 2H]$); 948.7 (pep-$H_1N_1F_1$; $[M + 2H]$); 1021.7 (pep-$H_1N_1F_2$; $[M + 2H]$);1058.6 (pep-H_2N_2; $[M + 2H]$); 1131.6 (pep-$H_2N_2F_1$; $[M + 2H]$); 1204.7 (pep-$H_2N_2F_2$)	WDLDPEVRPTSA	$H_2N_2F_3$
	1214.9 $[M + H + Na]^{2+}$	388.1 (H_1N_1); 534.1 ($H_1N_1F_1$); 552.1 (WDLD + $Na)^+$; 856.5 (y_8^*); 1059.7 (y_8^*-N); 1367.7 (y_8^*-$H_1N_1F_1$); 1570 (y_8^*-$H_1N_2F_1$); 1732.8 (y_8^*-$H_2N_2F_1$); 1878.8 (y_8^*-$H_2N_2F_2$)	WDLDPEVRPTSA	$H_2N_2F_2$
	1288.2 $[M + H + Na]^{2+}$	388.0 (H_1N_1); 534.1 ($H_1N_1F_1$); 552.1 (WDLD + Na); 680.2 ($H_1N_1F_2$); 856.5 (y_8^*); 1059.5 (y_8^*-N); 1367.7 y_8-$H_1N_1F_1$); 1716.7 (y_8^*-$H_1N_2F_2$); 1732.7 (y_8^*-$H_2N_2F_1$); 1878.9 (y_8^*-$H_2N_2F_2$); 2024.9 (y_8^*-$H_2N_2F_3$)	WDLDPEVRPTSA	$H_2N_2F_3$
22828	1040.8 $[M + 3H]^{3+}$	No fragmentation	WDLDPEVRPTSAVAA	$H_4N_2F_3$
22830	1040.8 $[M + 3H]^{3+}$	350.1 (N_1F_1); 366.1 (H_1N_1); 528.2 (H_2N_1); 674.2 ($H_2N_1F_1$); 820.3 ($H_2N_2F_2$); 814.1 (pep; $[M + 2H]$); 915.7 (pep-N_1; $[M + 2H]$); 1069.6 (pep-H_1N_1F; $[M + 2H]$); 1077.8 (pep-H_2N_1; $[M + 2H]$); 1150.9 (pep-$H_2N_1F_1$; $[M + 2H]$); 1179.5 (pep-N_2H_2; $[M + 2H]$); 1224.1 (pep-$H_2N_1F_2$; $[M + 2H]$); 1252.2 (pep-$H_2N_2F_2$; $[M + 2H]$); 1260.6 (pep-N_2H_3; $[M + 2H]$); 1326.0 (pep-$H_2N_2F_2$; $[M + 2H]$); 1341.6 (pep-N_2H_4; $[M + 2H]$); 1345.1 (pep-$H_3N_2F_1$; $[M + 2H]$); 1407.0 (pep-$H_3N_2F_2$; $[M + 2H]$); 1414.0 (pep-$N_2H_4F_1$; $[M + 2H]$); 1480.6 (pep- $H_3N_2F_3$; $[M + 2H]$); 1487.6 (pep-$H_4N_2F_2$ $[M + 2H]$); 1560.6 (pep-$H_4N_2F_3$ $[M + 2H]$)	WDLDPEVRPTSAVAA	$H_4N_2F_3$

[a] See Refs. 22–25.

ative for the $H_1N_1F_1$ composition, probably representing the other arm of the branched structure. However, this ion may also result from fragmentation of the larger arm. After the loss of three Fuc residues, two HexNAc residues, and one Hex residue, the branched structure gives rise to the signal at *m/z* 1098.4 $[M + H]^+$, which has a composition of N_2H_1-pep (where pep is the peptide moiety) and points toward a core 2 type *O*-glycosylation. Taken together, this CID MS/MS spectrum indicates that the composition of the glycan moiety is $H_2N_4F_3$. The fragmentation data support the sequence Fuc_2-($HexNAc_1$-Hex_1-$HexNAc_1$)-[Fuc_1-($HexNAc_1$-Hex_1)]-$HexNAc_1$. The monosaccharide identity and linkage positions of the individual carbohydrate units cannot be derived from the MS/MS spectrum. Differentiation between GalNAc and GlcNAc residues and linkage information are assigned on the basis of current knowledge of human *O*-glycosylation. We assume that a GalNAc is directly linked to the peptide moiety, whereas the other core HexNAc residue is a GlcNAc, and the hexose residues are assumed to be Gal, together forming the core 2 GlcNAcβ1–6Gal(β1–3)GalNAc motif. In contrast, the outer HexNAc residues of this glycopeptide may represent GalNAc or GlcNAc residues.

Based on the glycan composition, the peptide backbone mass was deduced to be 1627.0 $[M + H]^+$. We did not observe a substantial number of fragments that could be assigned to peptide backbone cleavages. This is a known phenomenon in ion trap CID MS/MS of glycopeptides (19–21). Therefore, MS^3 experiments of the fragment at *m/z* 814.0 within the MS/MS spectrum were performed, but only a clear fragment at *m/z* 1097.5 was observed, and the quality of the resulting spectrum was insufficient to identify the peptide backbone (data not shown).

Identification of Aberrantly Glycosylated Human Apolipoprotein C-III Peptides in Urine of S. mansoni-infected Individuals—Having identified a highly fucosylated glycopeptide in urine from a heavily infected individual in our comparative, global screen, we decided to perform a preparative purification of these urinary glycopeptides using 5 ml of urine. The SCX fractions containing the glycopeptides of interest were subsequently fractionated using HILIC HPLC, and fractions were analyzed by MALDI-TOF MS. Fig. 3*A* shows the spectrum from the fraction containing, among others, the above mentioned peptide at *m/z* 3201.6. The MALDI-TOF-TOF mass spectrum of this glycopeptide (Fig. 3*B*) showed a fragment at *m/z* 1626.7 $[M + H]^+$. As described above, we predicted this to be the mass of the peptide backbone. Moreover, the fragment at *m/z* 1097.5 that was observed in the MS^3 analysis of the putative peptide backbone (see above) was also evident in this spectrum, indicating peptide backbone cleavages during MALDI-TOF-TOF fragmentation.

The MALDI-TOF mass spectrum revealed masses that potentially correspond to truncated peptides (missing Ala, AA, or VAA) carrying an identical glycan structure. MALDI-TOF-TOF analysis of the peptides at *m/z* 3130.6 and 2960.4 confirmed this prediction (Fig. 3*B*) because the mass of the fragments containing the peptide backbone shifted accordingly (from 1626.7 to 1555.6 and 1385.9, respectively). The glycopeptide at *m/z* 2611.3 $[M + H]^+$ was interpreted as having the same peptide backbone as the peptide at *m/z* 2960.4 $[M + H]^+$ lacking one Fuc_1-$HexNAc_1$ element (Fig. 3*B*). The MALDI-TOF-TOF mass spectrum of the glycopeptide at *m/z* 3232.6 also revealed a fragment at *m/z* 1626.7. This indicates that the primary structure of the peptide backbone is the same as for the major species at *m/z* 3201.6, but the nature of the 31-Da mass difference remains elusive.

To identify the peptide backbone from the glycopeptides purified from urine from *S. mansoni*-infected individuals using SCX and HILIC HPLC, a high quality MALDI-TOF-TOF mass spectrum (Fig. 4*A*) from the most abundant glycopeptide (*m/z* 3201.6) was accumulated. This spectrum was used for manual interpretation, taking into account all the structural information obtained so far.

As mentioned above, the mass of the peptide backbone was predicted to be 1626.7 $[M + H]^+$. We reasoned that the fragment at *m/z* 1097.5 was the result of a cleavage at a labile bond within the peptide backbone, such as N-terminal of a proline and/or C-terminal of an aspartic acid. The fragment at *m/z* 2672.9 represents the same peptide fragment carrying the full glycan structure. The ions at *m/z* 530.0 and *m/z* 1097.5 would form a pair of b* and y* ions (* indicating ions without the glycan moiety) arising from the fragmentation of one specific peptide bond. Similarly, a pair is formed by the ions at *m/z* 616.1 and 1011.3.

Assuming that the 1097.5 is a y^*_n ion N-terminal of a proline and that the ion at 871.4 is the y^*_{n-2} generates the tag Pro-Glu. Following this line of reasoning, the mass difference between 871.4 and 616.1 could correspond to RV/VR, but because of the ion at 755.2, the most plausible tag would then be Pro-Glu-Val-Arg with the aforementioned 755.2 ion corresponding to $y^*_{n-3} - NH_3$. As discussed above, a set of glycopeptides corresponding to truncated peptides (lacking maximum AAV/VAA) was observed. Subsequently, BLAST searches using AAV*XX*(*X*)PEVR and PEVR*XXX*(*X*)VAA in the SchistoDB database (release 2.0; July 2008; 13,273 entries) were performed, but no peptide with full homology was identified. Therefore, partial matches were checked to see whether these could explain the generated MS data, but this approach also did not result in the identification of an *S. mansoni* peptide. As an alternative, BLAST searches in the human NCBInr database (released November 15, 2009; 225,299 entries) were performed, and surprisingly full homology with the C-terminal region of human apolipoprotein C-III (apoC-III; accession number GI:521205) was found using PEVR*XXXX*VAA as the search query (E-value, 119). Moreover, the C-terminal peptide WDLDPEVRPTSAVAA of apoC-III has a theoretical mass of 1626.8 $[M + H]^+$, nicely corresponding to what was predicted based on both the ion trap MS/MS data as well as the MALDI-TOF-TOF MS data. In addition,

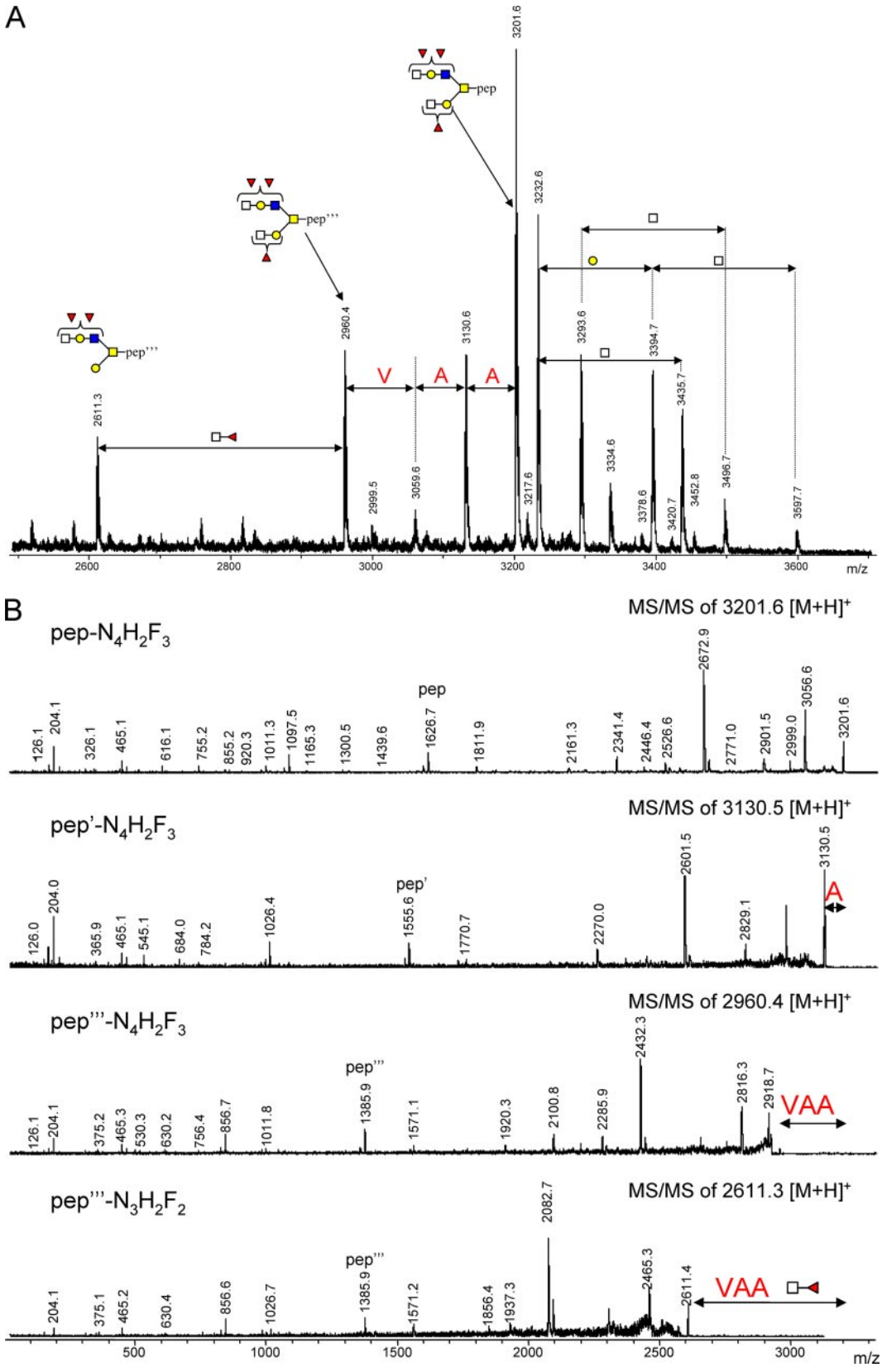

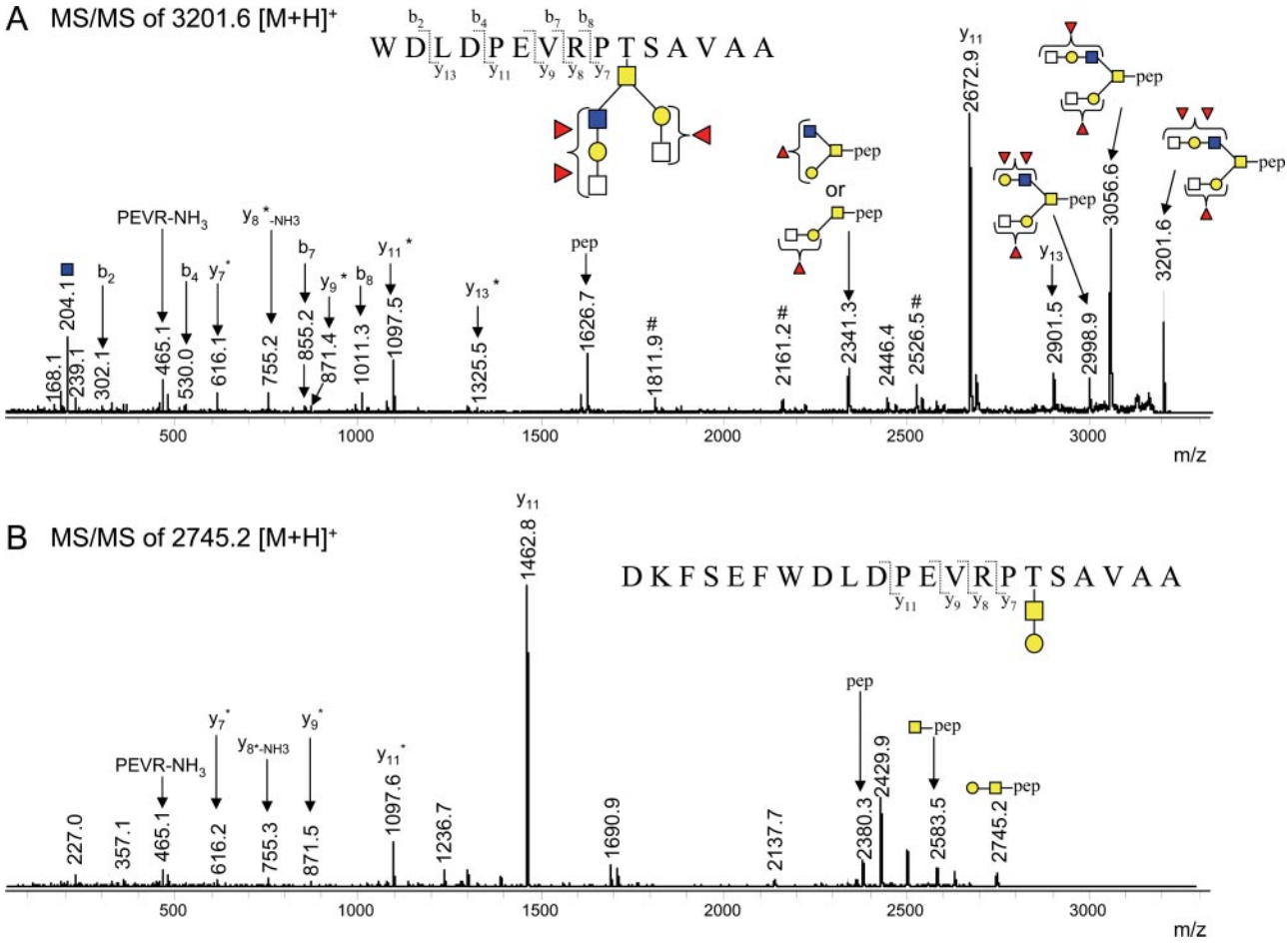

FIG. 4. **Highly fucosylated glycopeptides from urine of *S. mansoni*-infected individuals consist of C-terminal peptide of human apolipoprotein C-III.** *A*, MALDI-TOF-TOF analysis of the highly fucosylated glycopeptide at *m/z* 3201.6 ($[M + H]^+$) after SCX and normal phase purification of urinary peptides from an *S. mansoni*-infected individual. y ions indicated with * have lost the complete glycan moiety. Ions indicated with # are similar to y_{11} but have additionally lost one or more monosaccharides. *B*, normal human apolipoprotein C-III was digested with trypsin and analyzed with MALDI-TOF-TOF MS. Shown is a C-terminal tryptic glycopeptide containing one *N*-acetylgalactosamine-Gal element (corresponding to apoC-III_0). Note the similar series of y ions as observed in the MALDI-TOF-TOF spectrum in *A*. *Red triangle*, fucose; *yellow circle*, galactose; *blue square*, *N*-acetylglucosamine; *yellow square*, *N*-acetylgalactosamine; *open square*, *N*-acetylhexosamine. *pep*, peptide.

many of the theoretical y and b ions could be matched with this peptide sequence (Fig. 4*A*), and it also explains the MS/MS data of the truncated peptides (Fig. 3*B*).

Peptide WDLDPEVRPTSAVAA of apoC-III contains an *O*-glycosylation site at Thr^{74} within full-length apoC-III, which normally carries a core 1 mucin type *O*-glycan structure containing one galactose, one *N*-acetylgalactosamine, and zero, one, or two sialic acids (22–25). This heterogeneity in sialic acids is used in the nomenclature of the different human apoC-III isoforms, that is apoC-III_0, apoC-III_1, and apoC-III_2, respectively. Although we cannot formally exclude the possibility that the aberrantly glycosylated apoC-III peptide is glycosylated at Ser^{75}, we assume that it is also attached to Thr^{74}.

To further corroborate our assignment of the peptide moiety, purified commercially available human apolipoprotein C-III was digested with trypsin and analyzed with MALDI-TOF-(TOF) MS. As expected, a heterogeneous population of glycopeptides corresponding to the apoC-III_0, apoC-III_1, and

FIG. 3. **Preparative purification of glycopeptides from urine of *S. mansoni*-infected individual.** Urinary peptides from an *S. mansoni*-infected individual were separated using strong cation exchange chromatography. Fractions containing highly fucosylated glycopeptides were further purified using HILIC HPLC and measured by MALDI-TOF MS (*A*). In addition to the peptide at 3201.6 $[M + H]^+$ carrying $H_2N_4F_3$ (Fig. 2), truncated peptides (lacking Ala, Ala-Ala, or Val-Ala-Ala) with the same glycan moiety were detected. Moreover, heterogeneity in the glycan composition was observed. The heterogeneity in the peptide sequence and glycan moiety was confirmed by MALDI-TOF-TOF MS (*B*). *pep*, peptide; *pep′*, peptide lacking Ala; *pep‴*, peptide lacking Val-Ala-Ala. *Red triangle*, fucose; *yellow circle*, galactose; *blue square*, *N*-acetylglucosamine; *yellow square*, *N*-acetylgalactosamine; *open square*, *N*-acetylhexosamine.

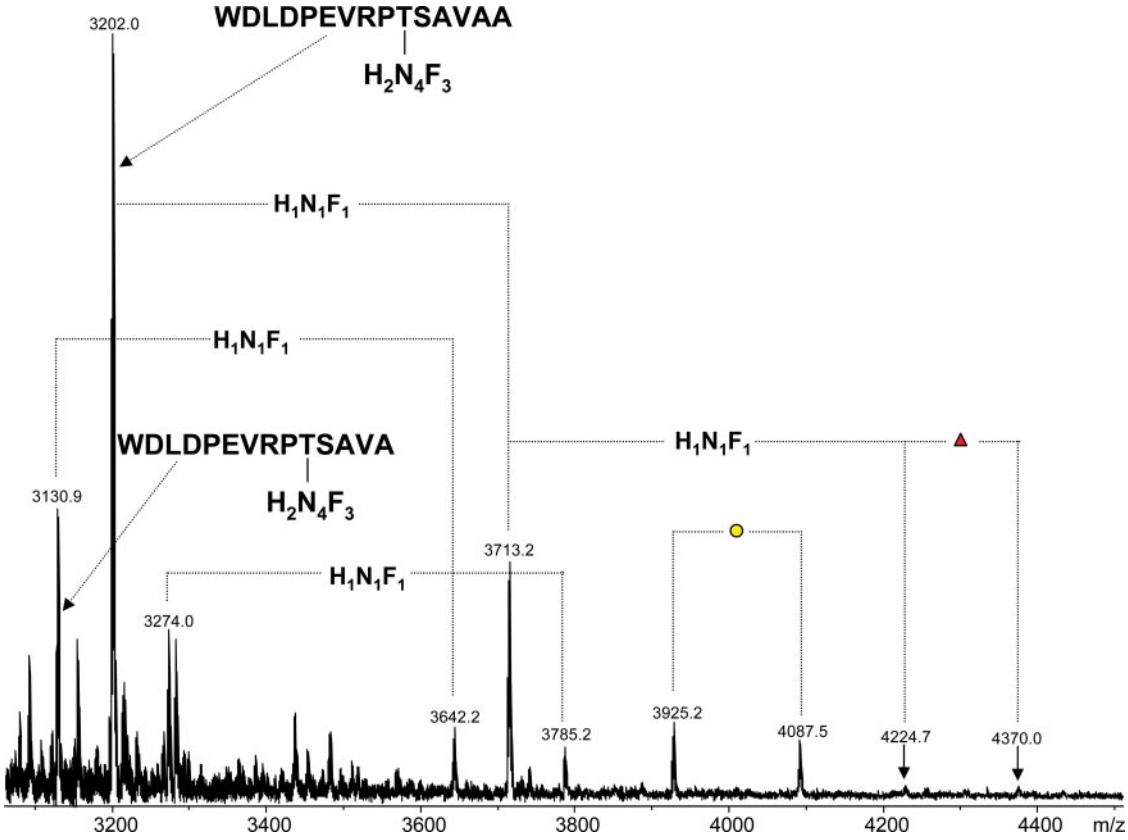

FIG. 5. **Aberrantly glycosylated apolipoprotein C-III-derived peptides from urine of *S. mansoni*-infected individuals contain multiple $H_1N_1F_1$ elements.** Urinary peptides from an *S. mansoni*-infected individual (10413) were separated using strong cation exchange chromatography. Fractions containing highly fucosylated glycopeptides were further purified using HILIC HPLC and measured by MALDI-TOF MS. Shown are the C-terminal apoC-III peptides WDLDPEVRPTSAVA(A) carrying $H_2N_4F_4$ but also one or two extra $H_1N_1F_1$ units. *Red triangle*, fucose; *yellow circle*, galactose.

apoC-III_2 isoforms was evident (data not shown). The MALDI-TOF-TOF mass spectrum from the C-terminal tryptic glycopeptide DKFSEFWDLDPEVRPT^{74}-($GalNAc_1$-Gal_1)SAVAA from apoC-III_0 (Fig. 4*B*) showed a similar mode of peptide backbone fragmentation as observed by MALDI-TOF-TOF MS of the major glycopeptide purified from urine of *S. mansoni*-infected individuals (Fig. 4*A*). This is most apparent for the y ion series because both peptides have the same C terminus but obviously differ at their N terminus. Specifically, the y_{11} ion is a prominent species in both spectra either with the glycan structure (*m/z* 1462.8 for apoC-III_0 and *m/z* 2672.9 for the urinary peptide) or without it (y^*_{11} at *m/z* 1097.5 in both spectra). Furthermore, the y^*_7, $y^*_8 - NH_3$, and y^*_9 ions are clearly distinguishable in both spectra. Altogether, in urine of an *S. mansoni*-infected individual, we identified apoC-III-derived glycopeptides carrying a glycan structure that is totally different from that of normal human apoC-III.

Aberrantly Glycosylated Apolipoprotein C-III Peptides Are Exclusively Identified in S. mansoni-infected Individuals—As a next step, all the selected urines (four controls and six infected) were similarly analyzed. All LC-MS runs were manually inspected for the presence of highly fucosylated glycopeptides containing the peptide backbone from the C terminus of apoC-III. Importantly, in none of the control samples were such glycopeptides identified (Table I). Fragmentation spectra corresponding to highly fucosylated apoC-III peptides were present in five of the six urines from *S. mansoni*-infected individuals. We used the information from the fragmentation patterns of the individual glycopeptides to predict the glycan composition and the peptide backbone (Table I). All these glycans differ drastically from the known glycan composition of human apoC-III. In total, they represent a very heterogeneous population of glycopeptides at both the peptide level and the glycan level. In one of the infected samples (22828), a mass corresponding to an aberrantly glycosylated peptide with an *m/z* and retention time similar to those of the one identified in sample 22830 was found, but it was not selected for MS/MS analysis and therefore not unambiguously identified (Table I). Purified glycopeptides from sample 10413 were also analyzed in the higher *m/z* range using MALDI-TOF MS. This revealed the presence of species containing one or two additional Hex_1-$HexNAc_1$-Fuc_1 units compared with the glycopeptide at *m/z* 3202.0 (Fig. 5). These units may represent additional Lewis X moieties (Galβ1→4(Fucα1→3)GlcNAcβ1),

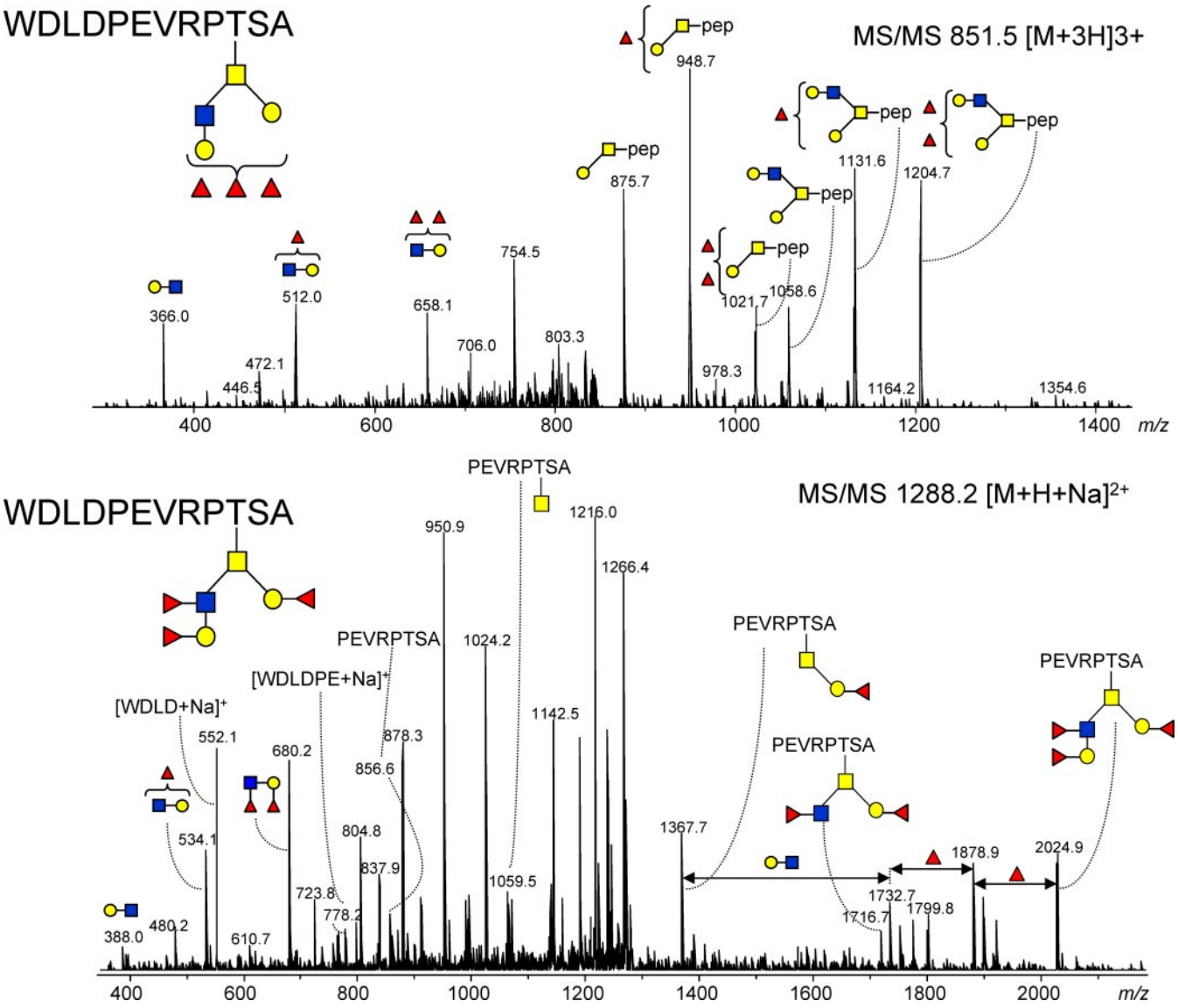

FIG. 6. **Characterization of fucose positions on aberrantly glycosylated apoC-III.** Urinary peptides from an *S. mansoni*-infected individual (22824) were separated using strong cation exchange chromatography. Fractions containing glycopeptides were analyzed using LC-ion trap MS, and glycopeptides were fragmented using collisional-induced dissociation. From one specific aberrantly glycosylated apoC-III peptide (WDLDPEVRPTSA carrying $H_2N_2F_3$), CID MS/MS spectra were recorded from a fully protonated (*A*) and partially sodiated (*B*) species. Within the MS/MS spectrum from the fully protonated species, a $[Fuc_2\text{-}Hex_1\text{-}HexNAc_1 + H]^+$ element was observed (*m/z* 658.1) potentially harboring a difucosyl (Fuc(α1–2)Fuc-) element. Subsequent fragmentation of the partially sodiated precursor indicated that no difucosyl elements were present. *Red triangle*, fucose; *yellow circle*, galactose; *blue square*, *N*-acetylglucosamine; *yellow square*, *N*-acetylgalactosamine. *pep*, peptide.

possibly as Lewis X tandem repeats. Moreover, starting from *m/z* 4224.7, a mass increase of 146 at *m/z* 4370.0 ($H_4N_6F_6$) corresponding to an additional fucose element was evident. Similarly, one putative extra Lewis X unit was noticed also for the truncated glycopeptide at *m/z* 3130.9 (lacking the C-terminal Ala).

We then analyzed samples containing the smaller peptides and glycan structures to gain more insight in the fucose positions. In one of the samples (22824), the apoC-III peptide WDLDPEVRPTSA containing the glycans $H_2N_2F_2$ and $H_2N_2F_3$ was found (Table I). In the MS/MS spectrum of the glycopeptide containing two fucoses (*m/z* 1204.2 $[M + 2H]^{2+}$), a singly charged ion corresponding to the peptide backbone with and without a HexNAc (*m/z* 1588.6 and 1385.5, respectively) was clearly present (Table I and supplemental material). The fragment ion pattern obtained from the protonated precursor (*m/z* 851.5 $[M + 3H]^{3+}$) of the glycopeptide containing one extra fucose (Fig. 6, *top*) revealed highly abundant singly charged glycan-specific oxonium ions at *m/z* 366.0 ($[Hex_1\text{-}HexNAc_1 + H]^+$), 512.0 ($[Fuc_1\text{-}Hex_1\text{-}HexNAc_1 + H]^+$), and 658.1 ($[Fuc_2\text{-}Hex_1\text{-}HexNAc_1 + H]^+$). It is well known that fucoses can easily transfer during mass spectrometric frag-

mentation of protonated ions, which may lead to misinterpretation of fragmentation spectra (26). Therefore, a fragmentation spectrum of the sodiated precursor $[M + H + Na]^{2+}$ at *m/z* 1288.2 (Fig. 6, *bottom*) was recorded. This showed similar singly charged glycan-specific sodium adduct ions at *m/z* 388.0 $[Hex_1\text{-}HexNAc_1 + Na]^+$, 534.1 $[Fuc_1\text{-}Hex_1\text{-}HexNAc_1 + Na]^+$, and 680.2 ($[Fuc_2\text{-}Hex_1\text{-}HexNAc_1 + Na]^+$). Interestingly, in this MS/MS spectrum, some peptide cleavages were evident, most prominently at the labile Asp-Pro bond, similar to MALDI-TOF-TOF fragmentation. For example, at *m/z* 552.1 $[M + Na]^+$, the b ion representing the sodiated peptide fragment WDLD is shown with the corresponding y_8 ion at *m/z* 2024.9. These fragments again verify the peptide identity as a fragment of apolipoprotein C-III. Furthermore, the signals at *m/z* 1716.7 $[M + H]^+$, *m/z* 1367.7 $[M + H]^+$, *m/z* 1059.5 $[M + H]^+$, and *m/z* 856.6 $[M + H]^+$ show the consecutive loss of $Fuc_1\text{-}Hex_1$, $Fuc_1\text{-}HexNAc_1$, $Fuc_1\text{-}Hex_1$, and HexNAc elements from the y_8 ion. Altogether, we observed a complex mixture of fucosylated termini, part of which could be explained by the presence of Lewis X and Lewis Y (Fucα1→2Galβ1→4(Fucα1→3)GlcNAcβ1) structural elements.

Analysis of Full-length ApoC-III in Serum from Infected and Non-infected Individuals—To study whether the aberrantly glycosylated apoC-III can be detected also in serum from *S. mansoni*-infected individuals, full-length apoC-III glycoforms in serum of infected and non-infected individuals were analyzed by MALDI-TOF MS (Fig. 7). A clear shift in the relative amount of non-, single, and double sialylated apoC-III (apoC-III_0, apoC-III_1, and apoC-III_2) in infected *versus* non-infected individuals was found. Most prominently, the ratio C-III_2/C-III_0 is higher in infected than in non-infected individuals. However, in these analyses no full-length apoC-III glycoforms carrying fucosylated elements similar to those observed in the glycopeptides in the urine of infected individuals were identified.

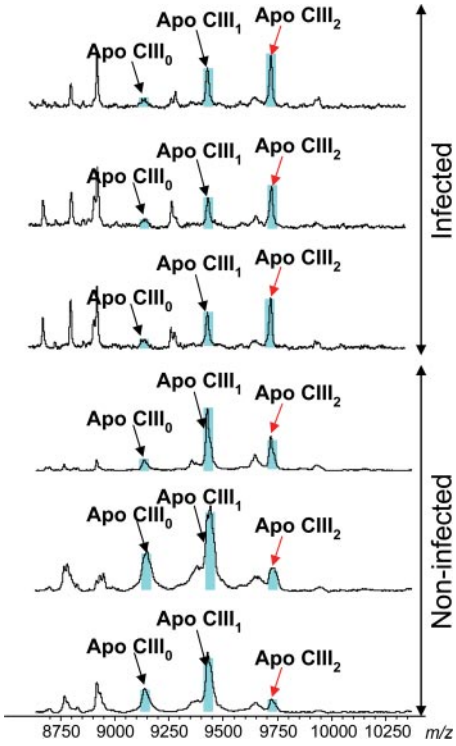

FIG. 7. **Profiling of apolipoprotein C-III glycoforms in serum of *S. mansoni*-infected and non-infected individuals.** Proteins were extracted from human serum samples from non-infected and *Schistosoma mansoni*-infected individuals using C_{18} ZipTips. Apolipoprotein C-III glycoforms in the eluates were measured by MALDI-TOF MS. A clear difference between the profile of the different apoC-III glycoforms in infected and non-infected individuals is apparent.

DISCUSSION

Mass spectrometry has become an indispensable tool for the characterization of glycopeptides and the analysis of protein glycosylation. Using this technology, we identified and characterized a set of human apolipoprotein C-III peptides aberrantly glycosylated at the *O*-glycosylation site (Thr^{74}) in urine of *S. mansoni*-infected individuals.

Although many methods based on mass spectrometric characterization of protein glycosylation are available, they are primarily suited for the analysis of *N*-linked glycans (27). The identification and structural characterization of *N*-glycosylation are simplified by the fact that it is usually part of a consensus sequence and by the availability of broad spectrum enzymes for the release of *N*-glycans. It is apparent that the characterization of *O*-glycosylated peptides, at the level of the glycan structure as well as of the peptide backbone, is much more challenging, particularly when the protein under investigation is unknown (21, 28–30). By combining different chromatographic techniques with various mass spectrometric analyses, we succeeded to characterize novel human apoC-III-derived *O*-glycosylated peptides. The glycan structures of these peptides are completely different from those described previously for apoC-III that consist of one galactose, one *N*-acetylgalactosamine, and zero, one, or two sialic acids (23, 25). In contrast, non-sialylated but highly fucosylated core 2 *O*-glycosylated peptides were identified from the urine samples.

ApoC-III is a small (79-amino acid) protein synthesized primarily in the liver and to a lesser extent in the intestine. It is an essential constituent of circulating particles rich in triacylglycerol, very low density lipoproteins, and high density lipoprotein. ApoC-III inhibits the hydrolysis of triglyceride-rich particles by the lipoprotein lipase (31). As a result, overexpression of apoC-III is associated with hypertriglyceridemia (32, 33) and atherosclerosis (34). Glycosylation on Thr^{74} of apoC-III has been well described (23, 35) but is not necessary for its secretion or lipid binding (36). Changes in the profile of the different apoC-III glycoforms analyzed with isoelectric focusing are used to identify *O*-glycan biosynthesis defects (37).

Currently, it is unclear what the relation is between aberrant apoC-III glycosylation, as described in this study, and *S. mansoni* infection. *S. mansoni* lacks a homologous apoC-III

gene (38), and we found no homologous peptide in the *S. mansoni* sequence database using a BLAST search with the identified peptide sequence, indicating that the novel apoC-III glycoforms we found in *S. mansoni* infection urine are of human origin. It may be hypothesized, however, that the modified apoC-III glycosylation is due to the action of the schistosomal glycosylation machinery. Some of the multifucosylated glycan structures present on the C-terminal peptide of the schistosomiasis-correlated apoC-III glycoforms seem to contain Lewis X elements. Multiple Lewis X elements are commonly found in *S. mansoni*, for example as part of CCA (39), indicating that the glycosylation machinery of the schistosome might be capable of synthesizing the type of glycan we identified on apoC-III. Such an action would require that the host-derived apoC-III is taken up by the schistosome and processed by the action of schistosomal glycosidases and glycosyltransferases. Although this would be a highly speculative hypothesis, it is not unlikely that schistosomes take up host-derived apoC-III. *S. mansoni* flukes cannot synthesize sterols and free fatty acids, and they acquire these from their host. How this is accomplished is still enigmatic, but binding of low density lipoproteins to the schistosome tegument has been shown (40), and several (very) low density lipoprotein-like receptors have been identified within the genome of *S. mansoni* (38). It is noteworthy that human schistosomiasis is frequently accompanied by dyslipoproteinemia and influences the development of atherosclerosis (41–45). Besides being a nutrient source providing the parasite with cholesterol and other lipids, surface binding of lipoproteins to various *Schistosoma* life stages may inhibit binding of anti-schistosome antibodies (46, 47) that may be part of the immune evasion process that underlies survival of the parasite.

Nevertheless, the fucosylated glycan elements identified on the apoC-III peptides in this study are not uncommon in other human glycoproteins (48–50). Moreover, profound effects on liver function and architecture are caused by immunopathological reactions to schistosome eggs deposited in the liver of the infected individual. Therefore, it seems plausible that aberrant glycosylation of liver apoC-III can be caused by changes in the glycosylation activity in the liver due to schistosomiasis-induced reactions. This interpretation is supported by the fact that we observed changes in the profile of the common apoC-III glycoforms, resulting in higher levels of the doubly sialylated form and lower levels of the non-sialylated glycoform. We have not observed full-length fucosylated apoC-III glycoforms, which might be the source of the presence of aberrantly urinary glycosylated peptides, in serum of infected individuals. This may be due to the relatively low levels of these forms in the serum or might have been the result of our methodology, which was developed to measure the common apoC-III glycoforms (18). Furthermore, the high level of heterogeneity in aberrant glycosylation, as observed on the urinary peptides, complicates straightforward identification of the full-length apoC-III equivalents.

Changes in the ratio of apoC-III glyco-isoforms have also been demonstrated in other diseases (51). Moreover, changes in the glycosylation of (serum) proteins in general have been observed in a variety of liver diseases (52). Interestingly, hyperfucosylation is one of the common alterations observed under these circumstances (53, 54). Consequently, it might be that aberrant glycosylation as described in this study is also present in other liver disorders. Studies with a larger cohort, including not only urine samples of schistosomiasis patients with different infection levels but also of patients with other liver diseases, could give more insight in the potential of the glycopeptides identified in this study as novel morbidity markers of (certain) liver disorders or as specific and sensitive markers of *Schistosoma* infection.

In conclusion, this study identified novel aberrantly glycosylated apoC-III peptides in urine of *S. mansoni*-infected individuals. Future studies will have to demonstrate the specificity of this phenomenon for this parasitic infection and to unravel the role of both *S. mansoni* and human factors. This will provide new insights in the molecular changes that are associated with *S. mansoni* infection.

Acknowledgments—We thank Dr. Govert van Dam for providing the samples and the parasitological information regarding *S. mansoni* infection and Carolien Koeleman for expert technical assistance. We give special thanks to all partners of the program, especially to Dr. Birgitte Vennervald, for the excellent coordination.

* This work was supported by the European Union Sixth Framework Program (Multi-Disciplinary Studies of Human Schistosomiasis in Uganda, Kenya and Mali: New Perspectives on Morbidity, Immunity, Treatment and Control (MUSTSchistUKEMA), Contract 517733).

S This article contains a supplemental ion trap CID MS/MS spectrum of aberrantly glycosylated apoC-III peptide WDLDPEVRPTSA carrying $H_2N_2F_2$ (*m/z* 1204.2, $[M + 2H]^{2+}$).

‡ To whom correspondence should be addressed. Tel.: 31-71-5269389; Fax: 31-71-5266907; E-mail:C.I.A.Balog@lumc.nl.

REFERENCES

1. Hotez, P. J., and Kamath, A. (2009) Neglected tropical diseases in sub-Saharan Africa: review of their prevalence, distribution, and disease burden. *PLoS Negl. Trop. Dis.* **3,** e412
2. Cheever, A. W., Hoffmann, K. F., and Wynn, T. A. (2000) Immunopathology of schistosomiasis mansoni in mice and men. *Immunol. Today* **21,** 465–466
3. Pearce, E. J., and MacDonald, A. S. (2002) The immunobiology of schistosomiasis. *Nat. Rev. Immunol.* **2,** 499–511
4. Hokke, C. H., Deelder, A. M., Hoffmann, K. F., and Wuhrer, M. (2007) Glycomics-driven discoveries in schistosome research. *Exp. Parasitol.* **117,** 275–283
5. Eberl, M., Langermans, J. A., Vervenne, R. A., Nyame, A. K., Cummings, R. D., Thomas, A. W., Coulson, P. S., and Wilson, R. A. (2001) Antibodies to glycans dominate the host response to schistosome larvae and eggs: Is their role protective or subversive? *J. Infect. Dis.* **183,** 1238–1247
6. Nyame, A. K., Lewis, F. A., Doughty, B. L., Correa-Oliveira, R., and Cummings, R. D. (2003) Immunity to schistosomiasis: glycans are potential antigenic targets for immune intervention. *Exp. Parasitol.* **104,** 1–13
7. Everts, B., Perona-Wright, G., Smits, H. H., Hokke, C. H., van der Ham, A. J., Fitzsimmons, C. M., Doenhoff, M. J., van der Bosch, J., Mohrs, K., Haas, H., Mohrs, M., Yazdanbakhsh, M., and Schramm, G. (2009) Omega-1, a glycoprotein secreted by Schistosoma mansoni eggs, drives Th2 responses. *J. Exp. Med.* **206,** 1673–1680
8. Hokke, C. H., and Yazdanbakhsh, M. (2005) Schistosome glycans and

innate immunity. *Parasite Immunol.* **27,** 257–264
9. Van de Vijver, K. K., Deelder, A. M., Jacobs, W., Van Marck, E. A., and Hokke, C. H. (2006) LacdiNAc- and LacNAc-containing glycans induce granulomas in an in vivo model for schistosome egg-induced hepatic granuloma formation. *Glycobiology* **16,** 237–243
10. De Jonge, N., Gryseels, B., Hilberath, G. W., Polderman, A. M., and Deelder, A. M. (1988) Detection of circulating anodic antigen by ELISA for seroepidemiology of Schistosomiasis mansoni. *Trans. R. Soc. Trop. Med. Hyg.* **82,** 591–594
11. De Jonge, N., Rabello, A. L., Krijger, F. W., Kremsner, P. G., Rocha, R. S., Katz, N., and Deelder, A. M. (1991) Levels of the schistosome circulating anodic and cathodic antigens in serum of schistosomiasis patients from Brazil. *Trans. R. Soc. Trop. Med. Hyg.* **85,** 756–759
12. Robijn, M. L., Koeleman, C. A., Wuhrer, M., Royle, L., Geyer, R., Dwek, R. A., Rudd, P. M., Deelder, A. M., and Hokke, C. H. (2007) Targeted identification of a unique glycan epitope of Schistosoma mansoni egg antigens using a diagnostic antibody. *Mol. Biochem. Parasitol.* **151,** 148–161
13. Robijn, M. L., Planken, J., Kornelis, D., Hokke, C. H., and Deelder, A. M. (2008) Mass spectrometric detection of urinary oligosaccharides as markers of Schistosoma mansoni infection. *Trans. R. Soc. Trop. Med. Hyg.* **102,** 79–83
14. van Dam, G. J., Wichers, J. H., Ferreira, T. M., Ghati, D., van Amerongen, A., and Deelder, A. M. (2004) Diagnosis of schistosomiasis by reagent strip test for detection of circulating cathodic antigen. *J. Clin. Microbiol.* **42,** 5458–5461
15. Katz, N., Coelho, P. M., and Pellegrino, J. (1970) Evaluation of Kato's quantitative method through recovery of Schistosoma mansoni eggs added to human feces. *J. Parasitol.* **56,** 1032–1033
16. Stelma, F. F., Talla, I., Polman, K., Niang, M., Sturrock, R. F., Deelder, A. M., and Gryseels, B. (1993) Epidemiology of Schistosoma mansoni infection in a recently exposed community in northern Senegal. *Am. J. Trop. Med. Hyg.* **49,** 701–706
17. Stelma, F. F., Talla, I., Verle, P., Niang, M., and Gryseels, B. (1994) Morbidity due to heavy Schistosoma mansoni infections in a recently established focus in northern Senegal. *Am. J. Trop. Med. Hyg.* **50,** 575–579
18. Nelsestuen, G. L., Zhang, Y., Martinez, M. B., Key, N. S., Jilma, B., Verneris, M., Sinaiko, A., and Kasthuri, R. S. (2005) Plasma protein profiling: unique and stable features of individuals. *Proteomics* **5,** 4012–4024
19. Deguchi, K., Ito, H., Baba, T., Hirabayashi, A., Nakagawa, H., Fumoto, M., Hinou, H., and Nishimura, S. I. (2007) Structural analysis of O-glycopeptides employing negative- and positive-ion multi-stage mass spectra obtained by collision-induced and electron-capture dissociations in linear ion trap time-of-flight mass spectrometry. *Rapid Commun. Mass Spectrom.* **21,** 691–698
20. Wu, S. L., Hühmer, A. F., Hao, Z., and Karger, B. L. (2007) On-line LC-MS approach combining collision-induced dissociation (CID), electron-transfer dissociation (ETD), and CID of an isolated charge-reduced species for the trace-level characterization of proteins with post-translational modifications. *J. Proteome Res.* **6,** 4230–4244
21. Wuhrer, M., Catalina, M. I., Deelder, A. M., and Hokke, C. H. (2007) Glycoproteomics based on tandem mass spectrometry of glycopeptides. *J. Chromatogr. B Analyt. Technol. Biomed. Life Sci.* **849,** 115–128
22. Brewer, H. B., Jr., Shulman, R., Herbert, P., Ronan, R., and Wehrly, K. (1974) Complete amino acid sequence of alanine apolipoprotein (ApoC-III). Apolipoprotein from human plasma very low-density lipoproteins. *J. Biol. Chem.* **249,** 4975–4984
23. Ito, Y., Breslow, J. L., and Chait, B. T. (1989) Apolipoprotein C-III$_0$ lacks carbohydrate residues: use of mass spectrometry to study apolipoprotein structure. *J. Lipid Res.* **30,** 1781–1787
24. Ueda, K., Fukase, Y., Katagiri, T., Ishikawa, N., Irie, S., Sato, T. A., Ito, H., Nakayama, H., Miyagi, Y., Tsuchiya, E., Kohno, N., Shiwa, M., Nakamura, Y., and Daigo, Y. (2009) Targeted serum glycoproteomics for the discovery of lung cancer-associated glycosylation disorders using lectin-coupled ProteinChip arrays. *Proteomics* **9,** 2182–2192
25. Vaith, P., Assmann, G., and Uhlenbruck, G. (1978) Characterization of the oligosaccharide side chain of apolipoprotein C-III from human plasma very low density lipoproteins. *Biochim. Biophys. Acta* **541,** 234–240
26. Wuhrer, M., Koeleman, C. A., Hokke, C. H., and Deelder, A. M. (2006) Mass spectrometry of proton adducts of fucosylated N-glycans: fucose transfer between antennae gives rise to misleading fragments. *Rapid Commun. Mass Spectrom.* **20,** 1747–1754
27. Wuhrer, M., Deelder, A. M., and Hokke, C. H. (2005) Protein glycosylation analysis by liquid chromatography-mass spectrometry. *J. Chromatogr. B Analyt. Technol. Biomed. Life Sci.* **825,** 124–133
28. Van den Steen, P. E., Rudd, P. M., Wormald, M. R., Dwek, R. A., and Opdenakker, G. (2000) O-Linked glycosylation in focus. *Trends Glycosci. Glycotechnol.* **12,** 35–49
29. Alving, K., Paulsen, H., and Peter-Katalinic, J. (1999) Characterization of O-glycosylation sites in MUC2 glycopeptides by nanoelectrospray QTOF mass spectrometry. *J Mass Spectrom.* **34,** 395–407
30. Peter-Kataliniæ, J. (2005) Methods in enzymology: O-glycosylation of proteins. *Methods Enzymol.* **405,** 139–171
31. Wang, C. S., McConathy, W. J., Kloer, H. U., and Alaupovic, P. (1985) Modulation of lipoprotein-lipase activity by apolipoproteins: effect of apolipoprotein C-III. *J. Clin. Investig.* **75,** 384–390
32. Ito, Y., Azrolan, N., O'Connell, A., Walsh, A., and Breslow, J. L. (1990) Hypertriglyceridemia as a result of human apo CIII gene expression in transgenic mice. *Science* **249,** 790–793
33. Cohn, J. S., Tremblay, M., Batal, R., Jacques, H., Rodriguez, C., Steiner, G., Mamer, O., and Davignon, J. (2004) Increased apoC-III production is a characteristic feature of patients with hypertriglyceridemia. *Atherosclerosis* **177,** 137–145
34. Kawakami, A., and Yoshida, M. (2009) Apolipoprotein CIII links dyslipidemia with atherosclerosis. *J. Atheroscler. Thromb.* **16,** 6–11
35. Maeda, H., Hashimoto, R. K., Ogura, T., Hiraga, S., and Uzawa, H. (1987) Molecular cloning of a human apoC-III variant: Thr-74—-Ala-74 mutation prevents O-glycosylation. *J. Lipid Res.* **28,** 1405–1409
36. Roghani, A., and Zannis, V. I. (1988) Mutagenesis of the glycosylation site of human ApoCIII. O-Linked glycosylation is not required for ApoCIII secretion and lipid binding. *J. Biol. Chem.* **263,** 17925–17932
37. Wopereis, S., Grünewald, S., Huijben, K. M., Morava, E., Mollicone, R., van Engelen, B. G., Lefeber, D. J., and Wevers, R. A. (2007) Transferrin and apolipoprotein C-III isofocusing are complementary in the diagnosis of N- and O-glycan biosynthesis defects. *Clin. Chem.* **53,** 180–187
38. Berriman, M., Haas, B. J., LoVerde, P. T., Wilson, R. A., Dillon, G. P., Cerqueira, G. C., Mashiyama, S. T., Al-Lazikani, B., Andrade, L. F., Ashton, P. D., Aslett, M. A., Bartholomeu, D. C., Blandin, G., Caffrey, C. R., Coghlan, A., Coulson, R., Day, T. A., Delcher, A., DeMarco, R., Djikeng, A., Eyre, T., Gamble, J. A., Ghedin, E., Gu, Y., Hertz-Fowler, C., Hirai, H., Hirai, Y., Houston, R., Ivens, A., Johnston, D. A., Lacerda, D., Macedo, C. D., McVeigh, P., Ning, Z., Oliveira, G., Overington, J. P., Parkhill, J., Pertea, M., Pierce, R. J., Protasio, A. V., Quail, M. A., Rajandream, M. A., Rogers, J., Sajid, M., Salzberg, S. L., Stanke, M., Tivey, A. R., White, O., Williams, D. L., Wortman, J., Wu, W., Zamanian, M., Zerlotini, A., Fraser-Liggett, C. M., Barrell, B. G., and El-Sayed, N. M. (2009) The genome of the blood fluke Schistosoma mansoni. *Nature* **460,** 352–358
39. Van Dam, G. J., Bergwerff, A. A., Thomas-Oates, J. E., Rotmans, J. P., Kamerling, J. P., Vliegenthart, J. F., and Deelder, A. M. (1994) The immunologically reactive O-linked polysaccharide chains derived from circulating cathodic antigen isolated from the human blood fluke Schistosoma mansoni have Lewis X as repeating unit. *Eur. J. Biochem.* **225,** 467–482
40. Tempone, A. J., Bianconi, M. L., and Rumjanek, F. D. (1997) The interaction of human LDL with the tegument of adult Schistosoma mansoni. *Mol. Cell. Biochem.* **177,** 139–144
41. Dimenstein, R., Carvalho, V. C., Oliveira, D. N., and Gillett, M. P. (1992) Alterations in the levels and lipid composition of plasma lipoproteins (VLDL, LDL and HDL) in Brazilian patients with hepatosplenic Schistosomiasis mansoni. *Braz. J. Med. Biol. Res.* **25,** 1091–1102
42. Lima, V. L., Sena, V. L., Stewart, B., Owen, J. S., and Dolphin, P. J. (1998) An evaluation of the marmoset Callithrix jacchus (sagui) as an experimental model for the dyslipoproteinemia of human Schistosomiasis mansoni. *Biochim. Biophys. Acta* **1393,** 235–243
43. Stanley, R. G., Jackson, C. L., Griffiths, K., and Doenhoff, M. J. (2009) Effects of Schistosoma mansoni worms and eggs on circulating cholesterol and liver lipids in mice. *Atherosclerosis* **207,** 131–138
44. Doenhoff, M. J., Stanley, R. G., Griffiths, K., and Jackson, C. L. (2002) An anti-atherogenic effect of Schistosoma mansoni infections in mice associated with a parasite-induced lowering of blood total cholesterol. *Parasitology* **125,** 415–421

45. La Flamme, A. C., Harvie, M., Kenwright, D., Cameron, K., Rawlence, N., Low, Y. S., and McKenzie, S. (2007) Chronic exposure to schistosome eggs reduces serum cholesterol but has no effect on atherosclerotic lesion development. *Parasite Immunol.* **29,** 259–266
46. Chiang, C. P., and Caulfield, J. P. (1989) Human lipoprotein binding to schistosomula of Schistosoma mansoni: displacement by polyanions, parasite antigen masking, and persistence in young larvae. *Am. J. Pathol.* **135,** 1015–1024
47. Chiang, C. P., and Caulfield, J. P. (1989) The binding of human low-density lipoproteins to the surface of schistosomula of Schistosoma mansoni is inhibited by polyanions and reduces the binding of anti-schistosomal antibodies. *Am. J. Pathol.* **134,** 1007–1018
48. Morris, H. R., Dell, A., Easton, R. L., Panico, M., Koistinen, H., Koistinen, R., Oehninger, S., Patankar, M. S., Seppala, M., and Clark, G. F. (1996) Gender-specific glycosylation of human glycodelin affects its contraceptive activity. *J. Biol. Chem.* **271,** 32159–32167
49. Pang, P. C., Tissot, B., Drobnis, E. Z., Sutovsky, P., Morris, H. R., Clark, G. F., and Dell, A. (2007) Expression of bisecting type and Lewisx/Lewisy terminated N-glycans on human sperm. *J. Biol. Chem.* **282,** 36593–36602
50. Yu, S. Y., Yang, Z., Khoo, K. H., and Wu, A. M. (2009) Identification of blood group A/A-Le(b/y) and B/B-Le(b/y) active glycotopes co-expressed on the O-glycans isolated from two distinct human ovarian cyst fluids. *Proteomics* **9,** 3445–3462
51. Harvey, S. B., Zhang, Y., Wilson-Grady, J., Monkkonen, T., Nelsestuen, G. L., Kasthuri, R. S., Verneris, M. R., Lund, T. C., Ely, E. W., Bernard, G. R., Zeisler, H., Homoncik, M., Jilma, B., Swan, T., and Kellogg, T. A. (2009) O-Glycoside biomarker of apolipoprotein C3: responsiveness to obesity, bariatric surgery, and therapy with metformin, to chronic or severe liver disease and to mortality in severe sepsis and graft vs host disease. *J. Proteome Res.* **8,** 603–612
52. Blomme, B., Van Steenkiste, C., Callewaert, N., and Van Vlierberghe, H. (2009) Alteration of protein glycosylation in liver diseases. *J. Hepatol.* **50,** 592–603
53. Chambers, W., Thompson, S., Skillen, A. W., Record, C. O., and Turner, G. A. (1993) Abnormally fucosylated haptoglobin as a marker for alcoholic liver disease but not excessive alcohol consumption or nonalcoholic liver disease. *Clin. Chim. Acta* **219,** 177–182
54. Nakagawa, T., Uozumi, N., Nakano, M., Mizuno-Horikawa, Y., Okuyama, N., Taguchi, T., Gu, J., Kondo, A., Taniguchi, N., and Miyoshi, E. (2006) Fucosylation of N-glycans regulates the secretion of hepatic glycoproteins into bile ducts. *J. Biol. Chem.* **281,** 29797–29806